Enhanced production of 3,4-dihydroxybutyrate from xylose by engineered yeast via xylonate re-assimilation under alkaline condition

Yukawa, Takahiro ; Bamba, Takahiro ; Matsuda, Mami ; Yoshida, Takanobu ; Inokuma, Kentaro ; Kim, Jungyeon ; Won Lee, Jae ; Jin, Yong-Su ;…

(Citation)
Biotechnology and Bioengineering,120(2):511-523

(Issue Date)
2023-02

(Resource Type)
journal article

(Version)
Accepted Manuscript

Title:

Enhanced production of 3,4-dihydroxybutyrate from xylose by engineered yeast via xylonate re-assimilation under alkaline condition

Authors:

Takahiro Yukawa[a], E-mail: 188p016p@stu.kobe-u.ac.jp

Takahiro Bamba[a], E-mail: t.bamba@bear.kobe-u.ac.jp

Mami Matsuda[a,b], E-mail: matsuda_mami@harbor.kobe-u.ac.jp

Takanobu Yoshida[a], E-mail: t-yoshida@port.kobe-u.ac.jp

Kentaro Inokuma[a], E-mail: kinokuma@port.kobe-u.ac.jp

Jungyeon Kim[c, d] E-mail: jungyeon@illinois.edu

Jae Won Lee[c, d] E-mail: jlee762@illinois.edu

Yong-Su Jin[c, d] E-mail: ysjin@illinois.edu

Akihiko Kondo[a, b, e] E-mail: akondo@kobe-u.ac.jp

Tomohisa Hasunuma[a, b, e], E-mail: hasunuma@port.kobe-u.ac.jp

Affiliations

[a] Graduate School of Science, Technology and Innovation, Kobe University, 1-1 Rokkodai, Nada, Kobe 657-8501, Japan

[b] Engineering Biology Research Center, Kobe University, 1-1 Rokkodai, Nada, Kobe, 657-8501, Japan

[c] Department of Food Science and Human Nutrition, University of Illinois at Urbana-Champaign, Urbana, IL, USA.

[d] Carl R. Woese Institute for Genomic Biology, University of Illinois at Urbana-Champaign, Urbana, IL, USA.

[e] RIKEN Center for Sustainable Resource Science, 1-7-22 Suehiro-cho, Tsurumi-ku, Yokohama, Kanagawa 230-0045, Japan

Corresponding author

Tomohisa Hasunuma

Engineering Biology Research Center, Kobe University
1-1 Rokkodai, Nada, Kobe 657-8501, Japan
hasunuma@port.kobe-u.ac.jp

Funding

This work was funded by project P16009 (Development of production techniques for highly functional biomaterials using plant and other organism smart cells) and P20011 (Development of bio-derived product production technology that accelerates the realization of carbon recycling) from the New Energy and Industrial Technology Development Organization (NEDO). TH was also supported by Grant-in-Aid for Scientific Research (B) (JP21H01729) from the Japan Society for the Promotion of Science (JSPS). TY was supported by JSPS Grant-in-Aid for JSPS Fellows (JP21J10891).

Abstract

To realize lignocellulose-based bioeconomy, efficient conversion of xylose into valuable chemicals by microbes is necessary. Xylose oxidative pathways that oxidize xylose into xylonate can be more advantageous than conventional xylose assimilation pathways because of fewer reaction steps without loss of carbon and ATP. Moreover, commodity chemicals like 3,4-dihydroxybutyrate and 3-hydroxybutyrolactone can be produced from the intermediates of xylose oxidative pathway. However, successful implementations of xylose oxidative pathway in yeast have been hindered because of the secretion and accumulation of xylonate which is a key intermediate of the pathway, leading to low yield of target product. Here, high-yield production of 3,4-dihydroxybutyrate from xylose by engineered yeast was achieved through genetic and environmental perturbations. Specifically, 3,4-dihydroxybutyrate biosynthetic pathway was established in yeast through deletion of *ADH6* and overexpression of *yneI*. Also, inspired by the mismatch of pH between host strain and key enzyme of XylD, alkaline

fermentations (pH ≥ 7.0) were performed to minimize xylonate accumulation. Under the alkaline conditions, xylonate was re-assimilated by engineered yeast and combined product yields of 3,4-dihydroxybutyrate and 3-hydroxybutyrolactone resulted in 0.791 mol/mol-xylose, which is highest compared with previous study. These results shed light on the utility of the xylose oxidative pathway in yeast.

KEYWORDS

3,4-Dihydroxybutyrate, 3-Hydroxybutyrolactone, Xylonate assimilation, Xylose oxidative pathway, *Saccharomyces cerevisiae*

1 | INTRODUCTION

For the sustainable production of commodity chemicals, replacing petrochemical-based industry with renewable biomass-based bioconversion is becoming an important proposition. Traditionally, starch and sugarcane have been used as feedstocks for microbial fermentation to produce biochemicals. However, using human-edible portions of crops may result in social and ethical issues such as unstable supply and fluctuating prices of foods. Therefore, non-edible biomass has received increasing attention as sustainable feedstocks for developing next-generation biorefineries (Protzko et al., 2018; Sun et al., 2021; Wei et al., 2013). Especially, lignocellulosic biomass, mainly composed of 30-50 % glucose, 20-25 % xylose, is one of the most abundant feedstocks on earth (Lane et al., 2018).

Glucose and xylose can be converted into various of bio-derived compounds via a conventional xylose pathway (Lee et al., 2022). However, xylose fermentation by an engineered yeast strain was much inferior to glucose fermentation because of many limiting factors such as carbon catabolite repression by glucose, redox imbalances, and by-product formation (Kim et al., 2013). In addition, conventional xylose assimilation pathway, utilizing xylose isomerase and xylose reductase/xylitol dehydrogenase, require the use of ATP when the metabolite enter central metabolic pathways such as pentose phosphate pathway (PPP) and glycolysis (Shen et al., 2020).

Recently, a xylose oxidative pathway has been identified as a novel non-phosphorylative pathway in recombinant microbial strains (Watanabe et al., 2019) (Fig. 1). The xylose oxidative pathway does not require ATP for shunting xylose into central metabolism, and the pathway is independent of the inherent glycolysis and PPP (Shen et al., 2020). As shown in Fig. 1, xylose is oxidized into 2-keto-3-deoxy-xylonate (KDX) and further converted to either α-ketoglutarate via the Weimberg pathway (Weimberg, 1961), or pyruvate and glycolaldehyde via

93 the Dahms pathway (Dahms, 1974). The xylose oxidative pathway has a potential
94 to produce chemicals such as 3,4-dihydroxybutyrate (3,4-DHBA) (Wang et al.,
95 2017), 1,2,4-butanetriol (BT) (Yukawa et al., 2021), ethylene glycol, or glycolate
96 (Salusjärvi et al., 2017) from xylose (Fig. 1).

97 3,4-DHBA and its lactonized form 3-hydroxybutyrolactone (3-HBL) are
98 versatile chemicals as 3-HBL is listed as one of the top value-added biochemicals
99 in the report by U. S. Department of Energy (Werpy and Petersen, 2004). 3-HBL
100 can be polymerized to produce polyhydroxyalkanoates, and it can be used as
101 precursors for synthesizing chiral drugs (Dhamankar et al., 2014). The microbial
102 production of 3-HBL and 3,4-DHBA from glucose and glycolate in *E. coli* was
103 firstly reported in 2013 (Martin et al., 2013), and subsequently achieved 0.32 g/L
104 of 3-HBL and 0.70 g/L of 3,4-DHBA from solely 10 g/L glucose (Dhamankar et
105 al., 2014). However, multiple reaction steps and low substrate specificity of
106 enzymes resulted in low yields and the formation of many by-products
107 (Dhamankar et al., 2014). In contrast, 3,4-DHBA production from xylose is more
108 desirable because of the 100 % theoretical yield from xylose and its
109 independence from glucose metabolism (Shen et al., 2020). Previously, 3,4-
110 DHBA synthetic pathway from xylose was established in *E. coli* (Wang et al.,
111 2017), and the integration of a fusion enzyme consisting of KDX decarboxylase
112 (PpMdlC) and xylonate dehydratase (YagF) resulted in a titer of 7.71 g/L of 3,4-
113 DHBA from 20 g/L of xylose with a molar yield of 60 % (Liu et al., 2021) (Table
114 2).

115 The xylose oxidative pathway has been introduced into bacterial strains
116 such as *Escherichia coli* (Fujiwara et al., 2020) and *Corynebacterium glutamicum*
117 (Brüsseler et al., 2019). Also, resulting strain in previous study exhibit good
118 growth from xylose as a sole carbon source (Tai et al., 2016) and product titers
119 and yields (Bai et al., 2016; Choi et al., 2016) with xylonate re-assimilation

(Bañares et al., 2021). The yeast *S. cerevisiae* is also desirable host strain for producing cellulosic biochemicals due to its high tolerance to fermentation inhibitors and no bacteriophage infection (Hong and Nielsen, 2012; Sharma et al., 2022). Indeed, engineered yeast could be more suitable for the production of bio-based chemicals from pretreated and hydrolyzed biomass as compared to engineered *E. coli* (Bamba et al. 2019). On the other hand, the engineered yeast strains accumulated excessive amounts of xylonate in the medium without xylonate re-assimilation (Bamba et al., 2019, Salusjärvi et al., 2017). Xylonate converted from xylose was immediately released outside the yeast cells before conversion to KDX. As such, productions of target molecules by engineered *S. cerevisiae* strains were not impressive (Salusjärvi et al., 2017; Yukawa et al., 2021, Table 2). Notably, the engineered yeast strains could not grow on xylose as a carbon source via Weimberg pathway (Borgström et al., 2019). These studies indicate that more improvement is necessary to realize more efficient xylose conversion with less xylonate accumulation via oxidative xylose pathway in *S. cerevisiae*.

To relieve xylonate accumulation by engineered *S. cerevisiae* strain, the enhancement in the activity of *Caulobacter crescentus* XylD has been needed. For example, strain engineering is effective by deleting *BOL2*, encoding transcriptional repressor of iron regulon, to enhance cellular iron uptake into the yeast cells (Kumánovics et al., 2008). In addition to the deletion of *BOL2*, the overexpression of a truncated *TYW1* (*tTYW1*), which enhances iron uptake in yeast (Li et al., 2011), more improved *C. crescentus* XylD activity (Bamba et al., 2019). Although the combination of *BOL2* deletion with *tTYW1* overexpression further improved XylD activity *in vitro*, this genetic perturbation did not lead to a higher titer of BT (Bamba et al., 2019). Although an *in vitro* enzyme assay is a powerful tool to confirm the expression of an active enzymes, the improvement

of *in vitro* enzyme activity does not always guarantee increased expression of the pathway *in vivo* or product titers. This might be due to the differences in the reaction environments between *in vitro* and *in vivo*. Notably, although the optimal pH range of *C. crescentus* XylD activity is reported to be from pH 7.0 to 9.0 by *in vitro* assay (Andberg et al., 2016), *S. cerevisiae* strains harboring a xylose oxidative pathway were conventionally cultivated in a pH range lower than 6.0 because of the acidification of the fermentation medium by the multiple factors, for example, the use of ammonium ion as a nitrogen source (Hensing et al., 1995). In addition, the effects of pH on xylose oxidative pathway in yeast have not been reported yet.

Here, we demonstrated the cultivation of engineered *S. cerevisiae* with a xylose oxidative pathway under weak alkaline conditions can induce extracellular xylonate import to the cells, leading to the increase of the intracellular availability of KDX and 3,4-DHBA production from xylose. As a result, 3,4-DHBA and 3-HBL titer reached at 6.5 and 0.20 g/L from 10.9 g/L xylose with a total molar yield of 79.1 % without xylonate accumulation after 120 h fermentation. These results demonstrate an effective strategy to reduce the accumulation of intermediates for accelerating the biorefinery via the xylose oxidative pathway in yeast and provide a new insight into how heterologous pathway fluxes can be altered in a host strain through environmental perturbations.

2 | MATERIALS AND METHODS

2.1| Chemicals

Due to the commercial unavailability of (*R*)-3,4-DHBA, the 3,4-DHBA standard was prepared as described in the previous study (Martin et al., 2013). 3-HBL purchased from Alfa Aesar (Ward Hill, Massachusetts, USA). Xylonate and KDX were purchased from Toronto Research Chemicals (North York, Canada) and Sigma-Aldrich (St. Louis, MO, USA), respectively. In addition, unless otherwise

174 stated, all chemicals were purchased from Nacalai Tesque (Kyoto, Japan). 3,4-
175 Dihydroxybutanal (DHB) was identified by a capillary electrophoresis time-of-
176 flight mass spectrometry (CE-TOFMS) at *m/z* = 103.0391 due to the unavailability
177 of an authentic DHB standard.

178 **2.2 | Strains and plasmid constructions**

179 *E. coli* NovaBlue (Merck Millipore, Darmstadt, Germany) was used for plasmid
180 construction. All plasmids were constructed by using the In-fusion HD cloning kit
181 (Takara Bio USA, Mountain View, CA, USA), according to the recommended
182 protocol. Codon-optimized *C. crescentus xylB* and *xylD*, and *Lactococcus lactis*
183 *kdcA* for *S. cerevisiae* have been were previously obtained (Bamba et al., 2019).
184 Codon-optimized *E. coli yneI* and sf for *S. cerevisiae* was synthesized by Geneart
185 (Thermo Fisher Scientific, Waltham, MA, USA).

186 *S. cerevisiae* YPH499 (Stratagene, La Jolla, CA, USA) was used in this
187 study. All yeast strains used in this study and their descriptions are summarized
188 in Table 1. The details of plasmid and strain construction were specified in
189 Supplemental Text S1 and Text S2.

190 **2.3 | Shake-flask fermentation**

191 Shake flask fermentation was conducted in a 200-mL baffled Erlenmeyer flask as
192 described in the previous study (Bamba et al., 2019). Briefly, fermentation was
193 performed in 20 mL of the YPDX medium containing 10 g/L yeast extract, 20 g/L
194 Bactopeptone (Difco Laboratories),10 g/L glucose and 10 g/L xylose with an initial
195 OD_{600} = 5.0. The 1.0 mL culture was collected at every sampling point to
196 determine the amounts of metabolites.

197 **2.4 | Batch fermentation in bioreactor**

198 Batch fermentation was performed using Bio Jar.8 (ABLE Biott, Tokyo, Japan)
199 with an initial working volume of 100 mL. Yeast cells grown in 400 mL YPD
200 medium at 30 ºC were collected by centrifugation at 2,200×g for 5 min and

washed by 10 mL distilled water twice. The washed cells were inoculated into the medium with initial OD_{600} = 5.0. The medium was composed of 10 g/L yeast extract, 20 g/L Bactopeptone, 10 g/L glucose and 10 g/L xylose at 0 h. Antifoam SI (FUJIFILM Wako Pure Chemical, Ltd., Osaka, Japan) was appropriately added. The temperature was controlled at 30 °C. The pH of culture was maintained by the automatic addition of a 5 N NaOH or 5N KOH. The airflow was maintained at 100 mL/min with compressed air. The culture medium was sampled every 24 h, to determine metabolite concentrations and cell density (OD_{600}) using a spectrophotometer.

2.5 | Metabolite analysis

The amounts of xylonate, BT, 3,4-DHBA and 3-HBL in the medium were analyzed by GC-MS (GCMS-QP 2010 Ultra; Shimadzu, Kyoto, Japan), and the running condition was described in the previous previously (Bamba et al., 2019).

Glucose and xylose concentrations in the medium were measured using high-performance liquid chromatography (HPLC) (Shimadzu, Kyoto, Japan) with a RID-10A refractive index detector (Shimadzu) equipped with an Eclipse XDB-C18 column (4.6 mm × 250 mm, particle size 5 μm; Agilent Technologies, Hercules, CA, USA). The HPLC system was operated at 80 °C, with a ultrapure water as the mobile phase at a flow rate of 0.6 mL/min.

CE-TOFMS (CE, Agilent G7100; MS, Agilent G6224AA LC/MSD TOF; Agilent Technologies, Palo Alto, CA, USA) was used to measure the amounts of intracellular xylonate, KDX, NAD^+, $NADP^+$ and extracellular KDX analysis. The method to extract metabolites from the medium (Yukawa et al., 2021) and cells (Inokuma et al., 2018), and running parameters (Hasunuma et al., 2013) was described in the previous reports.

pH in the fermentation medium was determined using compact pH meter (LAQUA twin, HORIBA, Kyoto, Japan). The method of intracellular pH analysis

was described previously (Reifenrath & Boles, 2018), specified in Supplemental Materials (Text S4).

3 | RESULTS AND DISCUSSION

3.1 | A pathway design to produce 3,4-dihydroxybutyrate from xylose in engineered yeast.

The 3,4-DHBA biosynthetic pathway from xylose is based on xylose oxidative pathway (Fig. 1). Xylose is converted into xylonolactone by xylose dehydrogenase XylB and xylonolactone is further converted into xylonate by the spontaneous reaction. Xylonate is then converted into KDX by xylonate dehydratase XylD, and KDX is catalyzed into 3,4-dihydroxybutanal (DHB) by 2-ketoacid decarboxylase. Previously, *Lactococcus lactis* KdcA is suitable for the decarboxylation of KDX to DHB (Bamba et al., 2019). Finally, DHB is converted into the 3,4-DHBA by aldehyde dehydrogenase (ALD). We first constructed the BDK strain harboring one copy of *C. crescentus* XylB, XylD, and *L. lactis* KdcA for the assessment of further study.

3.2 | Blocking the formation of by-product 1,2,4-butanetriol in engineered *yeast* through the knockout of alcohol dehydrogenase

To construct an efficient 3,4-DHBA biosynthetic pathway with high yield from xylose, the conversion of medium-chain aldehyde of DHB into a medium-chain alcohol BT by endogenous enzymes in yeast needs to be eliminated (Wang et al., 2017). Interruption of the reaction from DHB to yield BT would be critical because substantial amounts of BT were produced in the medium as a by-product by engineered *E. coli* (Wang et al., 2017). However, the enzymes responsible for catalyzing this reaction in *S. cerevisiae* have not been identified yet. In *S. cerevisiae*, Adh(s) catalyze the reversible reactions of aldehydes to alcohols such as well-characterized Adh1 to Adh7 (de Smidt et al., 2008). For example, Adh6 and Adh7 are known to exhibit broad substrate specificities

(Larroy et al., 2002a; Larroy et al., 2002b). Although substrate specificities of Adh(s) in *S. cerevisiae* have been investigated, no ADH(s) is known to recognize unnatural compounds such as DHB (Niu et al., 2003).

In order to reduce the formation of BT, we screened Adh(s) enzymes that might catalyze BT formation by disrupting each *ADH* genes in the BDK strain. To construct a *ADH* deletion library, each *ADH* gene from *ADH1* to *ADH7* was disrupted in the BDK strain, respectively. We performed glucose and xylose co-fermentation and examined the xylose consumption and BT production by the ADH disrupted strain (Fig. 2A and 2B). The parental BDK strain produced 0.22 g/L of BT from 10.6 g/L xylose at 96 h (Fig. 2A and 2B). Deletion of *ADH2, ADH5,* or *ADH7* did not change the titers of BT. Interestingly, the deletion of *ADH3* had a positive effect on BT production, and the BT titer reached 0.29 g/L after 96 h fermentation (Fig. 2B). In contrast, the deletion of *ADH1*, *ADH4*, and *ADH6* reduced the titers of BT after 96 h fermentation as compared with the parental BDK strain. In particular, the BDKΔ6 with the deletion of *ADH6* produced BT only at 0.01 g/L (Fig. 2B). Deletion of *ADH1* also reduced the xylose consumption (Fig. 2A), leading to the low BT production (Fig. 2B). Deletion of *ADH4* also reduced BT titer at 0.18 g/L (Fig. 2B). In particular, the titer of BT was dropped from 0.22 g/L of BDK strain to 0.01 g/L of BDKΔ6 strain at 96 h by the deletion of *ADH6* (Fig. 2B). These results suggest that *ADH6* is a deletion target for a high yield production of 3,4-DHBA by engineered yeast. However, the BDKΔ6 strain did not produce 3,4-DHBA. This suggested further engineering is required for 3,4-DHBA production.

3.3 | Increased fluxes from xylonate to 3,4-dihydroxybutanal enable the production of 3,4-dihydroxybutyrate in engineered yeast

Previously, we developed the BDδK603 strain for the production of BT (Yukawa et al., 2021). This strain harbors one copy of *C. crescentus* XylB and XylD, and

six copies of *L. lactis* KdcA. In addition, iron metabolism was modified with the deletion of *BOL2* and the overexpression of *tTYW1* to improve the activity of iron-sulfur protein XylD (Bamba et al., 2019; Yukawa et al., 2021). As the BDδK603 strain exhibits higher fluxes from xylose to DHB (Yukawa et al., 2021), we reasoned that the deletion of *ADH6* in the BDδK603 strain might enable the production of 3,4-DHBA from xylose.

To minimize BT formation while keeping the flux of xylose to DHB in the BDδK603 strain, *ADH6 gene* was deleted in the genome of the BDδK603 strain, resulting in the construction of the BDδK604 strain. We examined the product profiles from glucose and xylose fermentation by the parental BDδK603 strain and *ADH6*-deleted BDδK604 strains. The BDδK603 strain produced 7.4 g/L of xylonate (Fig. S1) and 1.5 g/L of BT (Fig. 2C). Interestingly, the BDδK603 strain produced 0.3 g/L of 3,4-DHBA without the deletion of any *ADH(s)* or integration of ALD catalyzing the reaction from DHB to 3,4-DHBA (Fig. 2D). By the disruption of *ADH6*, the BDδK604 strain produced 8.2 g/L of xylonate (Fig. S1), 0.3 g/L of BT (Fig. 2C), and 0.4 g/L of 3,4-DHBA (Fig. 2D). While the deletion of *ADH6* reduced BT formation from 1.5 to 0.3 g/L of BT (Fig. 2C), the improvement of 3,4-DHBA production was marginal (Fig. 2D, 0.3 vs. 0.4 g/L of 3,4-DHBA) between the BDδK603 and BDδK604 strains. The molar yield of 3,4-DHBA in BDδK604 strain was only 0.02 %. While endogenous aldehyde dehydrogenase in yeast might be converting DHB to 3,4-DHBA (Fig. 2D), heterologous enzyme needs to be introduced into the BDδK604 strain for the enhanced production of 3,4-DHBA.

3.4 | Improvement of 3,4-dihydroxybutyrate production by integration of suitable aldehyde dehydrogenase

As the structure of DHB is similar to that of succinate semialdehyde, succinate semialdehyde dehydrogenase YneI from *E. coli* was overexpressed to the increased production of the 3,4-DHBA by engineered *E. coli* (Wang et al., 2017).

309 Thus, the *yneI* was selected as a target gene for the enhanced production of 3,4-
310 DHBA in *S. cerevisiae*. In addition, we reasoned that endogenous enzymes in *S*
311 *cerevisiae* such as succinate semialdehyde dehydrogenase of Uga2, NAD^+-
312 dependent cytoplasmic ALDs of Ald2 and Ald3 might be responsible for the small
313 amounts of 3,4-DHBA produced by the BDδK603 and BDδK604 strains (Fig. 2D).
314 Therefore, Uga2, Ald2, and Ald3 were additionally selected as candidate
315 enzymes for 3,4-DHBA production.

316 Each gene of *yneI*, *UGA2*, *ALD2* and *ALD3* under the control of *TDH3*
317 promoter was integrated into the BDδK604 strain, resulting in the construction of
318 the BDδK604-YneI, BDδK604-Uga2, BDδK604-Ald2 and BDδK604-Ald3 strains,
319 respectively. As shown in Fig. 3A, the overexpression of *yneI* enhanced 3,4-
320 DHBA production at 1.0 g/L from 10.6 g/L of consumed xylose (Fig. S2) with a
321 molar yield of 11.8 %, which was 2.5-fold higher than the parental strain BDδK604
322 at 0.4 g/L (Fig. 2D). The overexpression of *UGA2* did not improve the 3,4-DHBA
323 titer. The overexpression of *ALD2* and *ALD3* also enhanced the carbon flux
324 toward 3,4-DHBA, producing 0.7 and 0.5 g/L of 3,4-DHBA by the BDδK604-Ald2
325 and BDδK604-Ald3 strains, respectively. These results suggested that YneI is
326 the most effective ALD among the overexpressed enzymes.

327 Xylonate accumulation by these strains changed marginally, but the
328 overexpression of *yneI* relieved xylonate accumulation at 8.2 g/L (Fig. 3B). This
329 means that 66.5% of the consumed xylose was wasted into the medium as
330 xylonate, resulting in the low yield of 3,4-DHBA from xylose by the BDδK604-
331 YneI strain. BT formation by the BDδK604-YneI strain was slightly lower as
332 compared with those by the other strains, and intracellular pH values and the pool
333 size of intracellular NAD^+ and $NADP^+$ at 24 h did not exhibit significant differences
334 (Fig. S3). Thus, YneI might have a better substrate specificity for DHB between
335 the four enzymes. In addition to the change of metabolites, pH of the culture

medium of the BDδK604-YneI strain drastically dropped from pH = 6.3 at 0 h to pH = 4.0 at 96 h (Fig. 3C) because a major by-product xylonate is a weak acid and is known to acidify fermentation media (Toivari et al., 2012), and final product 3,4-DHBA is also weak acid with a pKa value of 4.09.

3.5 | The 3,4-dihydroxybutyrate production under the pH control

Control of oxygen supply and pH of culture media in a lab-scale shake-flask fermentation is difficult so that our fermentation results for the production of 3,4-DHBA might not reflect the full potential of the engineered BDδK604-YneI strains. As such, pH-controlled fermentation in a bioreactor were performed to examine the production capacity of 3,4-DHBA production by the BDδK604-YneI under different aeration conditions.

Using a bioreactor, fermentation was performed while keeping the lower limit of pH of the medium was kept at 6.0 by NaOH. The effects of aeration on the production of 3,4-DHBA by the BDδK604-YneI were evaluated through changing agitation speeds from 200 to 500 rpm. Dissolved oxygen levels were controlled corresponding to the agitation speeds (Fig. S4). Glucose was completely consumed within 24 h by each agitation speed (Fig. S5), and xylose was sequentially consumed in the fermentation at 500 rpm (Fig. 4A). 5.8 g/L of xylonate was accumulated (Fig. 4B) and 3.5 g/L of 3,4-DHBA was produced (Fig. 4C). Compared to the result at 500 rpm, fermentations at lower agitation speeds exhibited the reduced xylose consumption rates, less amounts of accumulated xylonate, and higher titers of 3,4-DHBA. Notably, the fermentation at 300 rpm produced 4.6 g/L of 3,4-DHBA with a molar yield of 51.3 % from 11.2 g/L of xylose. Increase in the production of 3,4-DHBA under low aeration conditions at 300 rpm would be due to the XylD activity. XylD is known to be IlvD/EDD protein family requires an iron-sulfur cluster for its activity (Andberg et al., 2016). Functional expression of prokaryotic iron-sulfur proteins in yeast *S. cerevisiae* has been so

difficult because of oxygen sensibility of iron-sulfur proteins (Kirby et al. 2016), or conceivably low availability of iron-sulfur cluster (Bamba et al. 2019). Lower agitation speeds might reduce the loss of function of XylD, leading to less xylonate accumulation and increased the production of 3,4-DHBA even with lower xylose consumption.

Importantly, 3-HBL was also produced from xylose by spontaneous cyclization at 0.64 (200 rpm), 0.49 (300 rpm), 0.40 (400 rpm), and 0.39 g/L (500 rpm) under each agitation speed, respectively (Fig. 4D). This is the first report of 3-HBL production from xylose in *S. cerevisiae*, to the best of our knowledge. The previous study showed the dual production of 3,4-DHBA and 3-HBL from glucose (Dhamankar et al., 2014), but did not confirm the production of 3-HBL from xylose (Gao et al., 2017; Liu et al., 2021; Wang et al., 2017).

3.6 | Xylonate re-assimilation led to enhanced 3,4-dihydroxybutyrate production by engineered yeast

The beneficial effects of the pH and agitation control on 3,4-DHBA production were confirmed. While xylonate accumulation reduced with the control of pH and aeration, 4.8 g/L of xylonate was still accumulated with the molar yield of 38.7 % of the consumed xylose. Previously, *C. crescetus* XylD activity was determined to be highly active under a weak alkaline condition at pH = 8.5 (Andberg et al., 2016). The optimal pH for XylD was narrow so that XylD activities drastically dropped when pH was lower than 8.5. However, in previous studies, engineered yeast strains harboring a xylose oxidative pathway with *C. crescentus* XylD have been empirically cultivated at pH ≤ 6.0 (Bamba et al., 2019; Borgström et al., 2019; Salusjärvi et al., 2017). As the intracellular pH of *S. cerevisiae* responds to the extracellular pH changes (Orij et al., 2009), traditional yeast fermentation at pH ≤ 6.0 might make XylD inactive in *S. cerevisiae*. A weak alkaline environment would enhance the heterologous XylD activity by elevating intracellular pH in *S.*

390 *cerevisiae*. However, the impacts of alkaline fermentation on xylose oxidative
391 metabolism in *S. cerevisiae* have never been investigated so far.
392 To resolve the pH mismatch between optimal yeast growth and XylD
393 activity, fermentations were performed while keeping a lower limit of pH in the
394 medium at pH ≥ 7.0 or pH ≥ 8.0 by NaOH or KOH. To control the pH in the
395 fermentation medium, NaOH or KOH was used. Glucose was consumed within
396 24 h under all fermentation conditions (Fig. 5A). On the other hand, xylose
397 consumption rates reduced when the pH was maintained at pH ≥ 8.0 as
398 compared to when the pH was maintained at pH ≥ 7.0 (Fig. 5B). Interestingly,
399 xylonate was re-assimilated from the medium into the cells under alkaline
400 conditions and completely re-assimilated after 120 h cultivation. (Fig. 5C). This is
401 the first observation of xylonate re-assimilation when using *S. cerevisiae* as a
402 host strain. In all fermentations conducted under alkaline conditions, the titers of
403 3,4-DHBA increased up to 6.5 g/L with a molar yield of 74.5 % from 10. 9 g/L of
404 xylose when pH was controlled at pH ≥ 8.0 using KOH (Fig. 5D). These results
405 indicated that the weak alkaline conditions might lead to the *in vivo* activation of
406 *C. crescentus* XylD, the re-assimilations of xylonate, and the increased
407 productions of 3,4-DHBA production. For the efficient construction of
408 heterologous pathway, researchers need to reconsider how heterologous
409 enzymes are expressed in active form inside the microbial cells by the matching
410 the optimal pH between host strain and target enzymes since the active pH range
411 of heterologous enzymes often differs from the optimal pH of microbial host
412 strains (Ahn et al., 2020). Unfortunately, 3-HBL production was decreased to 0.30
413 (NaOH, pH ≥ 7.0), 0.21 (NaOH, pH ≥ 8.0), 0.37 (KOH, pH ≥ 7.0), and 0.20 g/L
414 (KOH, pH ≥ 8.0) under alkaline conditions (Fig. S7). as compared to 0.49 g/L of
415 3-HBL in the fermentation conducted at pH ≥ 6.0 using NaOH (Fig. 4D).

To elucidate the detailed metabolome in the 3,4-DHBA synthetic pathway, the intracellular amounts of xylonate, KDX and DHB, and extracellular amounts of KDX were measured. The intracellular amount of xylonate did not change under each fermentation conditions except for the intracellular xylonate at pH ≥ 8.0 using KOH (Fig. 6A). In contrast, the intracellular levels of KDX and DHB were increased remarkably when the cells were cultured at pH ≥ 8.0 (Fig. 6B and 6C), which could be due to increased XylD activity dependent on the higher intracellular pH values. Indeed, lifting the pH in the medium from pH 6.0 to 8.0 led to the increase in intracellular pH values, and XylD activity was dependent on pH from 6.0 to 8.0 (Fig. S6). Consistent with the increased level of intracellular KDX, the extracellular amount of KDX was also increased when the cells were cultured at pH ≥ 7.0 or at pH ≥ 8.0 (Fig. 6D). This indicated that putative bottlenecks in the 3,4-DHBA biosynthetic pathway might be the reaction from KDX to DHB. The expression levels of the genes involved in the 3,4-DHBA synthetic pathway did not change by changing the pH to alkaline conditions except for *xylD* (Fig. S8). Hence, this would be caused by the mismatch of the optimal pH between enzymes. For example, the optimal pH of *L. lactis* KdcA is pH 6.0 (Yep et al., 2006), which is quite different from those of *C. cresrentus* XylB (pH 9.0) (Toivari et al., 2012), *C. cresrentus* XylD (pH 8.5) (Andberg et al., 2016). Although the pH dependency of *E. coli* YneI has not been reported, the enzyme is assayed at pH = 7.8 (Fuhrer et al., 2007). Thus, a weak alkaline environment would not be beneficial for all the reactions in the biosynthetic pathway.

When KOH was used as an alkaline reagent, xylonate accumulation was lower as compared to when NaOH was used (Fig. 5C). However, it did not have an impact on the 3,4-DHBA production. This might be caused by the low flux in the 3,4-DHBA biosynthetic pathway, leading to the accumulation of intermediates of KDX and DHB. After 72 h cultivation, intracellular levels of KDX and DHB when

KOH was used was 2.1- and 1.5-fold higher than those in the fermentation using NaOH at pH ≥ 7.0 (Fig. 6A and 6B). Moreover, KDX when using KOH was accumulated in the medium with 1.5-fold higher as compared to using NaOH (Fig. 6C). Thus, the flux in the 3,4-DHBA biosynthetic pathway needs to be improved for further study.

In addition to the effects of pH, transporters involved in facilitating the import or export across the yeast cell membranes need to be identified for further engineering. For example, *S. cerevisiae* transports weak carboxylic acids like acetate into the cells, and the Jen family proteins, belong to the major facilitator superfamily, are identified to associate with plasma membrane transport of weak carboxylic acids in yeast (Giannattasio et al., 2013). When proteins involved in the transport of DHB, KDX and 3,4-DHBA are identified, further engineering could realize more efficient production of 3,4-DHBA with less accumulation of the intermediates.

4 |CONCLUSIONS

This research demonstrated xylonate re-assimilation by engineered yeast for the first time. The alkaline environment is the trigger of xylonate re-assimilation, overcoming the low yields of a xylose derivative chemicals. Based on this study, we envision the implementation of a xylose oxidative pathway in yeast would be more accelerated and universally used to produce biofuels and biochemicals from lignocellulosic feedstock. Furthermore, these results provide new insights into the reduction and re-assimilation of intermediates, as well as how the heterologous pathway works in the host strain to match the active pH range of host strain and target enzyme.

REFERENCE

Ahn, J. H., Seo, H., Park, W., Seok, J., Lee, J. A., Kim, W. J., Kim, G. B., Kim, K.-J., & Lee, S. Y. (2020). Enhanced succinic acid production by *Mannheimia* employing optimal malate dehydrogenase. *Nature Communications, 11(1)*, 1970. https://doi.org/10.1038/s41467-020-15839-z

Andberg, M., Aro-Kärkkäinen, N., Carlson, P., Oja, M., Bozonnet, S., Toivari, M., Hakulinen, N., O'Donohue, M., Penttilä, M., & Koivula, A. (2016). Characterization and mutagenesis of two novel iron–sulphur cluster pentonate dehydratases. *Applied Microbiology and Biotechnology, 100(17)*, 7549–7563. https://doi.org/10.1007/s00253-016-7530-8

Bai, W., Tai, Y.-S., Wang, J., Wang, J., Jambunathan, P., Fox, K. J., & Zhang, K. (2016). Engineering nonphosphorylative metabolism to synthesize mesaconate from lignocellulosic sugars in *Escherichia coli. Metabolic Engineering, 38*, 285–292. https://doi.org/10.1016/j.ymben.2016.09.007

Bamba, T., Yukawa, T., Guirimand, G., Inokuma, K., Sasaki, K., Hasunuma, T., & Kondo, A. (2019). Production of 1,2,4-butanetriol from xylose by *Saccharomyces cerevisiae* through Fe metabolic engineering. *Metabolic Engineering, 56*, 17–27. https://doi.org/10.1016/j.ymben.2019.08.012

Bañares, A. B., Nisola, G. M., Valdehuesa, K. N. G., Lee, W.-K., & Chung, W.-J. (2021). Understanding D-xylonic acid accumulation: A cornerstone for better metabolic engineering approaches. *Applied Microbiology and Biotechnology, 105(13)*, 5309–5324. https://doi.org/10.1007/s00253-021-11410-y

Borgström, C., Wasserstrom, L., Almqvist, H., Broberg, K., Klein, B., Noack, S., Lidén, G., & Gorwa-Grauslund, M. F. (2019). Identification of modifications procuring growth on xylose in recombinant *Saccharomyces cerevisiae* strains carrying the Weimberg pathway. *Metabolic Engineering, 55*, 1–11. https://doi.org/10.1016/j.ymben.2019.05.010

Brüsseler, C., Späth, A., Sokolowsky, S., & Marienhagen, J. (2019). Alone at last! – Heterologous expression of a single gene is sufficient for establishing the five-step Weimberg pathway in *Corynebacterium glutamicum*. *Metabolic Engineering Communications, 9,* e00090. https://doi.org/10.1016/j.mec.2019.e00090

Calahorra, M., Martínez, G. A., Hernández-Cruz, A., & Peña, A. (1998). Influence of monovalent cations on yeast cytoplasmic and vacuolar pH. *Yeast, 14(6)*, 501–515. https://doi.org/10.1002/(SICI)1097-0061(19980430)14:6<501::AID-YEA249>3.0.CO;2-6

Choi, S. Y., Park, S. J., Kim, W. J., Yang, J. E., Lee, H., Shin, J., & Lee, S. Y. (2016). One-step fermentative production of poly(lactate-co-glycolate) from carbohydrates in Escherichia coli. *Nature Biotechnology, 34(4)*, 435–440. https://doi.org/10.1038/nbt.3485

Dahms, A.S., (1974). 3-Deoxy-D-pentulosonic acid aldolase and its role in a new pathway of D-xylose degradation. Biochem. Biophys. *Res. Commun. 60*, 1433–1439

de Smidt, O., du Preez, J. C., & Albertyn, J. (2008). The alcohol dehydrogenases of *Saccharomyces cerevisiae*: A comprehensive review. *FEMS Yeast Research, 8(7)*, 967–978. https://doi.org/10.1111/j.1567-1364.2008.00387.x

Dhamankar, H., Tarasova, Y., Martin, C. H., & Prather, K. L. J. (2014). Engineering E. coli for the biosynthesis of 3-hydroxy-γ-butyrolactone (3HBL) and 3,4-dihydroxybutyric acid (3,4-DHBA) as value-added chemicals from glucose as a sole carbon source. *Metabolic Engineering, 25*, 72–81. https://doi.org/10.1016/j.ymben.2014.06.004

Fuhrer, T., Chen, L., Sauer, U., & Vitkup, D. (2007). Computational Prediction and Experimental Verification of the Gene Encoding the NAD^+/$NADP^+$-Dependent Succinate Semialdehyde Dehydrogenase in *Escherichia coli*. *Journal of Bacteriology, 189(22)*, 8073–8078. https://doi.org/10.1128/JB.01027-07

522 Fujiwara, R., Noda, S., Tanaka, T., & Kondo, A. (2020). Metabolic engineering of
523 *Escherichia coli* for shikimate pathway derivative production from glucose–xylose
524 co-substrate. *Nature Communications, 11(1)*, 279.
525 https://doi.org/10.1038/s41467-019-14024-1
526 Gao, H., Gao, Y., & Dong, R. (2017). Enhanced biosynthesis of 3,4-
527 dihydroxybutyric acid by engineered *Escherichia coli* in a dual-substrate system.
528 *Bioresource Technology, 245*, 794–800.
529 https://doi.org/10.1016/j.biortech.2017.09.017
530 Giannattasio, S., Guaragnella, N., Ždralević, M., & Marra, E. (2013). Molecular
531 mechanisms of *Saccharomyces cerevisiae* stress adaptation and programmed
532 cell death in response to acetic acid. *Frontiers in Microbiology*, 4.
533 https://doi.org/10.3389/fmicb.2013.00033
534 Hasunuma, T., Kikuyama, F., Matsuda, M., Aikawa, S., Izumi, Y., & Kondo, A.
535 (2013). Dynamic metabolic profiling of cyanobacterial glycogen biosynthesis
536 under conditions of nitrate depletion. *Journal of Experimental Botany, 64(10)*,
537 2943–2954. https://doi.org/10.1093/jxb/ert134
538 Hensing, M. C. M., Bangma, K. A., Raamsdonk, L. M., de Hulster, E., van Dijken,
539 J. P., & Pronk, J. T. (1995). Effects of cultivation conditions on the production of
540 heterologous α-galactosidase by *Kluyveromyces lactis*. *Applied Microbiology and*
541 *Biotechnology, 43(1)*, 58–64. https://doi.org/10.1007/BF00170623
542 Hong, K.-K., & Nielsen, J. (2012). Metabolic engineering of *Saccharomyces*
543 *cerevisiae*: A key cell factory platform for future biorefineries. Cellular and
544 *Molecular Life Sciences, 69(16)*, 2671–2690. https://doi.org/10.1007/s00018-
545 012-0945-1
546 Inokuma, K., Matsuda, M., Sasaki, D., Hasunuma, T., & Kondo, A. (2018).
547 Widespread effect of N-acetyl-d-glucosamine assimilation on the metabolisms of

548 amino acids, purines, and pyrimidines in *Scheffersomyces stipitis*. *Microbial Cell*
549 *Factories, 17*. https://doi.org/10.1186/s12934-018-0998-4
550 Kim, S. R., Park, Y.-C., Jin, Y.-S., & Seo, J.-H. (2013). Strain engineering of
551 *Saccharomyces cerevisiae* for enhanced xylose metabolism. *Biotechnology*
552 *Advances, 31(6)*, 851–861. https://doi.org/10.1016/j.biotechadv.2013.03.004
553 Kirby, J., Dietzel, K. L., Wichmann, G., Chan, R., Antipov, E., Moss, N., Baidoo,
554 E. E. K., Jackson, P., Gaucher, S. P., Gottlieb, S., LaBarge, J., Mahatdejkul, T.,
555 Hawkins, K. M., Muley, S., Newman, J. D., Liu, P., Keasling, J. D., & Zhao, L.
556 (2016). Engineering a functional 1-deoxy-D-xylulose 5-phosphate (DXP) pathway
557 in *Saccharomyces cerevisiae*. *Metabolic Engineering,* 38, 494–503.
558 https://doi.org/10.1016/j.ymben.2016.10.017
559 Kumánovics, A., Chen, O. S., Li, L., Bagley, D., Adkins, E. M., Lin, H., Dingra, N.
560 N., Outten, C. E., Keller, G., Winge, D., Ward, D. M., & Kaplan, J. (2008).
561 Identification of *FRA1* and *FRA2* as Genes Involved in Regulating the Yeast Iron
562 Regulon in Response to Decreased Mitochondrial Iron-Sulfur Cluster Synthesis.
563 *Journal of Biological Chemistry, 283(16)*, 10276–10286.
564 https://doi.org/10.1074/jbc.M801160200
565 Lane, S., Dong, J., & Jin, Y.-S. (2018). Value-added biotransformation of
566 cellulosic sugars by engineered *Saccharomyces cerevisiae*. *Bioresource*
567 *Technology, 260*, 380–394. https://doi.org/10.1016/j.biortech.2018.04.013
568 Larroy, C., Fernández, M. R., González, E., Parés, X., & Biosca, J. A. (2002).
569 Characterization of the *Saccharomyces cerevisiae* YMR318C (*ADH6*) gene
570 product as a broad specificity NADPH-dependent alcohol dehydrogenase:
571 Relevance in aldehyde reduction. *Biochemical Journal, 361(Pt 1)*, 163–172.
572 Larroy, C., Parés, X., & Biosca, J. A. (2002). Characterization of a
573 *Saccharomyces cerevisiae* NADP(H)-dependent alcohol dehydrogenase
574 (ADHVII), a member of the cinnamyl alcohol dehydrogenase family. *European*

575 *Journal of Biochemistry, 269(22)*, 5738–5745. https://doi.org/10.1046/j.1432-
576 1033.2002.03296.x
577 Lee, Y., Kim, C., Sun, L., Lee, T., & Jin, Y. (2022). Selective production of retinol
578 by engineered *Saccharomyces cerevisiae* through the expression of retinol
579 dehydrogenase. *Biotechnology and Bioengineering, 119(2)*, 399–410.
580 https://doi.org/10.1002/bit.28004
581 Li, L., Jia, X., Ward, D. M., & Kaplan, J. (2011). Yap5 Protein-regulated
582 Transcription of the *TYW1* Gene Protects Yeast from High Iron Toxicity. The
583 *Journal of Biological Chemistry, 286(44)*, 38488–38497.
584 https://doi.org/10.1074/jbc.M111.286666
585 Liu, Y., Mao, X., Zhang, B., Lin, J., & Wei, D. (2021). Modification of an
586 engineered *Escherichia coli* by a combinatorial strategy to improve 3,4-
587 dihydroxybutyric acid production. *Biotechnology Letters, 43(10)*, 2035–2043.
588 https://doi.org/10.1007/s10529-021-03169-z
589 Martin, C. H., Dhamankar, H., Tseng, H.-C., Sheppard, M. J., Reisch, C. R., &
590 Prather, K. L. J. (2013). A platform pathway for production of 3-hydroxyacids
591 provides a biosynthetic route to 3-hydroxy-γ-butyrolactone. *Nature*
592 *Communications, 4(1)*. https://doi.org/10.1038/ncomms2418
593 Niu, W., Molefe, M. N., & Frost, J. W. (2003). Microbial Synthesis of the Energetic
594 Material Precursor 1,2,4-Butanetriol. 2.
595 Orij, R., Postmus, J., Ter Beek, A., Brul, S., & Smits, G. J. (2009). *In vivo*
596 measurement of cytosolic and mitochondrial pH using a pH-sensitive GFP
597 derivative in *Saccharomyces cerevisiae* reveals a relation between intracellular
598 pH and growth. *Microbiology, 155(1)*, 268–278.
599 https://doi.org/10.1099/mic.0.022038-0
600 Peña, A., Sánchez, N. S., Álvarez, H., Calahorra, M., & Ramírez, J. (2015).
601 Effects of high medium pH on growth, metabolism and transport in

Saccharomyces cerevisiae. *FEMS Yeast Research, 15(2)*. https://doi.org/10.1093/femsyr/fou005

Protzko, R. J., Latimer, L. N., Martinho, Z., de Reus, E., Seibert, T., Benz, J. P., & Dueber, J. E. (2018). Engineering *Saccharomyces cerevisiae* for co-utilization of d-galacturonic acid and d-glucose from citrus peel waste. *Nature Communications, 9(1)*. https://doi.org/10.1038/s41467-018-07589-w

Reifenrath, M., & Boles, E. (2018). A superfolder variant of pH-sensitive pHluorin for *in vivo* pH measurements in the endoplasmic reticulum. *Scientific Reports*, 8(1), 11985. https://doi.org/10.1038/s41598-018-30367-z

Salusjärvi, L., Toivari, M., Vehkomäki, M.-L., Koivistoinen, O., Mojzita, D., Niemelä, K., Penttilä, M., & Ruohonen, L. (2017). Production of ethylene glycol or glycolic acid from D-xylose in *Saccharomyces cerevisiae*. *Applied Microbiology and Biotechnology*, *101(22)*, 8151–8163. https://doi.org/10.1007/s00253-017-8547-3

Sharma, J., Kumar, V., Prasad, R., & Gaur, N. A. (2022). Engineering of *Saccharomyces cerevisiae* as a consolidated bioprocessing host to produce cellulosic ethanol: Recent advancements and current challenges. *Biotechnology Advances, 56*, 107925. https://doi.org/10.1016/j.biotechadv.2022.107925

Shen, L., Kohlhaas, M., Enoki, J., Meier, R., Schönenberger, B., Wohlgemuth, R., Kourist, R., Niemeyer, F., van Niekerk, D., Bräsen, C., Niemeyer, J., Snoep, J., & Siebers, B. (2020). A combined experimental and modelling approach for the Weimberg pathway optimization. *Nature Communications, 11(1)*, 1098. https://doi.org/10.1038/s41467-020-14830-y

Sun, L., Lee, J. W., Yook, S., Lane, S., Sun, Z., Kim, S. R., & Jin, Y.-S. (2021). Complete and efficient conversion of plant cell wall hemicellulose into high-value bioproducts by engineered yeast. *Nature Communications, 12(1)*, 4975. https://doi.org/10.1038/s41467-021-25241-y

629 Tai, Y.-S., Xiong, M., Jambunathan, P., Wang, J., Wang, J., Stapleton, C., &
630 Zhang, K. (2016). Engineering nonphosphorylative metabolism to generate
631 lignocellulose-derived products. *Nature Chemical Biology, 12(4)*, 247–253.
632 https://doi.org/10.1038/nchembio.2020
633 Toivari, M. H., Nygård, Y., Penttilä, M., Ruohonen, L., & Wiebe, M. G. (2012).
634 Microbial d-xylonate production. *Applied Microbiology and Biotechnology, 96(1)*,
635 1–8. https://doi.org/10.1007/s00253-012-4288-5
636 Toivari, M., Nygård, Y., Kumpula, E.-P., Vehkomäki, M.-L., Benčina, M.,
637 Valkonen, M., Maaheimo, H., Andberg, M., Koivula, A., Ruohonen, L., Penttilä,
638 M., & Wiebe, M. G. (2012). Metabolic engineering of *Saccharomyces cerevisiae*
639 for bioconversion of d-xylose to d-xylonate. *Metabolic Engineering, 14(4)*, 427–
640 436. https://doi.org/10.1016/j.ymben.2012.03.002
641 Wang, J., Shen, X., Jain, R., Wang, J., Yuan, Q., & Yan, Y. (2017). Establishing
642 a novel biosynthetic pathway for the production of 3,4-dihydroxybutyric acid from
643 xylose in *Escherichia coli*. *Metabolic Engineering, 41*, 39–45.
644 https://doi.org/10.1016/j.ymben.2017.03.003
645 Watanabe, S., Fukumori, F., Nishiwaki, H., Sakurai, Y., Tajima, K., & Watanabe,
646 Y. (2019). Novel non-phosphorylative pathway of pentose metabolism from
647 bacteria. *Scientific Reports, 9(1)*, 155. https://doi.org/10.1038/s41598-018-
648 36774-6
649 Wei, N., Quarterman, J., Kim, S. R., Cate, J. H. D., & Jin, Y.-S. (2013). Enhanced
650 biofuel production through coupled acetic acid and xylose consumption by
651 engineered yeast. *Nature Communications, 4(1)*, 2580.
652 https://doi.org/10.1038/ncomms3580
653 Weimberg, R., (1961). Pentose oxidation by *Pseudomonas fragi*. *J. Biol. Chem.*
654 *236*, 629–635.

Werpy, T., & Petersen, G. (2004). Top Value Added Chemicals from Biomass: Volume I -- Results of Screening for Potential Candidates from Sugars and Synthesis Gas (DOE/GO-102004-1992, 15008859). https://doi.org/10.2172/15008859

Yep, A., Kenyon, G. L., & McLeish, M. J. (2006). Determinants of substrate specificity in KdcA, a thiamin diphosphate-dependent decarboxylase. *Bioorganic Chemistry, 34(6)*, 325–336. https://doi.org/10.1016/j.bioorg.2006.08.005

Yukawa, T., Bamba, T., Guirimand, G., Matsuda, M., Hasunuma, T., & Kondo, A. (2021). Optimization of 1,2,4 - butanetriol production from xylose in *Saccharomyces cerevisiae* by metabolic engineering of NADH/NADPH balance. *Biotechnology and Bioengineering, 118(1)*, 175–185. https://doi.org/10.1002/bit.27560

Table captions:

Table 1 Strain used in the present study.

Table 2 The biochemical production by microorganisms via a xylose oxidative pathway

Figure captions:

Fig. 1

Overview of the xylose oxidative pathway. KDX, 2-Keto-3-deoxy-xylonate; AKGSA, α-Ketoglutarate semialdehyde; AKG, α-Ketoglutarate; EG, Ethylene glycol; DHB, 3,4-Dihydroxybutanal; 3,4-DHBA, 3,4-Dihydroxybutyrate; 3-HBL, 3-Hydroxybutylolactone; XylB, Xylose dehydrogenase; XylD, Xylonate dehydratase; XylX, 2-Keto-3-deoxy-xylonate dehydratase; XylA, α-Ketoglutarate semialdehyde dehydrogenase; YjhH and YagG, KDX aldolase, ALD, aldehyde dehydrogenase; ADH, alcohol dehydrogenase; Kdc, 2-ketoacid decarboxylase.

Fig. 2

The effects of ADH gene disruption on (A) xylose consumption and (B) BT production by the BDK (orange, dot circle), BDKΔ1(red, squares), BDKΔ2 (blue, rhombuses), BDKΔ3 (green, triangles), BDKΔ4 (purple, crosses), BDKΔ5 (light yellow, bars) BDKΔ6 (black, circles), BDKΔ7 (brown, asterisks) with disruption of each ADH gene. (C) The time-course profiles of BT production and (D) 3,4-DHBA production during the glucose and xylose co-fermentation by the BDδK603 (control, green triangles) and BDδK604 (*ADH6* deletion, red squares) strains. The fermentation medium contained 10 g/L glucose and 10 g/L xylose. Error bars indicate standard deviations from three independent experiments.

Fig. 3

The time-course profiles of (A) 3,4-DHBA production and (B) xylonate accumulation by engineered *S. cerevisiae* strains expressing different ALDs. BDδK604-YneI (blue, circles), BDδK604-Uga2 (orange, crosses), BDδK604-Ald2 (purple, triangles), and BDδK604-Ald3 (light yellow, asterisks). The shake-flask fermentations were performed in the YP medium containing 10 g/L glucose and 10 g/L of xylose. (C) Time-course of pH change during the fermentation of BDδK604-YneI (green). The optimal pH range of *S. cerevisiae* for growth is shown in grey range. Error bars indicate standard deviations from three independent experiments.

Fig. 4

The effects of different agitation rates on (A) xylose consumption, (B) xylonate accumulation, and (C) 3,4-DHBA production by the BDδK604-YneI strain under the pH control using a bioreactor. Agitation speeds were changed at 200 rpm (orange, squares), 300 rpm (red, circles), 400 rpm (blue, rhombuses), and 500 rpm (green, triangles) at pH ≥ 6.0. (D) The 3-HBL productions by the BDδK604-YneI strain under the different agitation speeds (200 rpm, 300 rpm, 400 rpm, and 500 rpm) at pH ≥ 6.0. The engineered yeast was cultivated in the YP medium containing 10 g/L of glucose and 10 g/L of xylose, and the pH of fermentation medium was maintained at pH ≥ 6.0 using 5 N NaOH. Error bars indicate standard deviations from two independent experiments.

Fig. 5

Time-course profiles of (A) glucose consumption, (B) xylose consumption, (C) xylonate accumulation, and (D) 3,4-DHBA production by the BDδK604-YneI strain during the pH-controlled fermentation using a bioreactor. The

723 fermentations were performed under the alkaline conditions at pH ≥ 7.0 using
724 NaOH (orange, squares) and 8.0 using NaOH (red, rhombuses), or at pH ≥ 7.0
725 using KOH (blue, triangles), and 8.0 using KOH (green, circles) in the YP medium
726 containing 10 g/L of glucose and 10 g/L of xylose. Error bars indicate standard
727 deviations from two independent experiments.
728
729 **Fig. 6**
730 The amounts of (A) intracellular xylonate and (B) the relative amounts of
731 intracellular KDX, (C) intracellular DHB, and (D) extracellular KDX when re-
732 assimilating xylonate from the medium into the cells of the BDδK604-YneI strain.
733 The fermentations were performed at pH ≥ 7.0 or 8.0 using NaOH or KOH in the
734 YP medium containing 10 g/L of glucose and 10 g/L of xylose. Blue and orange
735 bar indicates the sample at 72 h and 96 h, respectively. The relative amounts
736 were shown as a fold change in the metabolites amount at 72 h at pH ≥ 6.0 by
737 NaOH. Error bars indicate standard deviations from two independent
738 experiments.
739

Strain Name	Description	Reference
YPH499	*MATa ura3 - 52 lys2 - 801 ade2 - 101 trp1 - 63 his3 - Δ200 le*	Stratagene
YPH499 ΔGRE3	YPH499, *gre3Δ::kanMX*	Bamba et al. 2019
BDK	YPH499, pTs-A-xylBD-kdcA	This study
BDKΔ1	BDK, *ADH1Δ::KanMX*	This study
BDKΔ2	BDK, *ADH2Δ::KanMX*	This study
BDKΔ3	BDK, *ADH3Δ::KanMX*	This study
BDKΔ4	BDK, *ADH4Δ::KanMX*	This study
BDKΔ5	BDK, *ADH5Δ::KanMX*	This study
BDKΔ6	BDK, *ADH6Δ::KanMX*	This study
BDKΔ7	BDK, *ADH7Δ::KanMX*	This study
BDδK603	YPH499 ΔGRE3, tdh3p-CcxylB, sed1p-CcxylD, six copies of *L. lactis kdcA* , *bol2Δ::HIS3* , pgk1p-tTYW1	Yukawa et al. 2021
BDδK604	BDδK603, *ADH6Δ::1 kbp fragment*	This study
BDδK604-YneI	BDδK604, pIL-tdh3p-Ec_yneI-adh1t	This study
BDδK604-Uga2	BDδK604, pIL-tdh3p-Sc_UGA2-adh1t	This study
BDδK604-Ald2	BDδK604, pIL-tdh3p-Sc_ALD2-adh1t	This study
BDδK604-Ald3	BDδK604, pIL-tdh3p-Sc_ALD3-adh1t	This study
YneI-sfpHluorin	BDδK604-YneI, pIU-pTDH3-sfpHluorin-tADH1	This study
Uga2-sfpHluorin	BDδK604-Uga2, pIU-pTDH3-sfpHluorin-tADH1	This study
Ald2-sfpHluorin	BDδK604-Ald2, pIL-pTDH3-sfpHluorin-tADH1	This study
Ald3-sfpHluorin	BDδK604-Ald3, pIL-pTDH3-sfpHluorin-tADH1	This study

Table 2 The biochemical production by microorganisms via a xylose oxidative pathway

Host	Carbon source	Target Products	Mode of culuture	Titer	Yield	Reference
Escherichia coli	20 g/L Xylose	3,4-DHBA	Batch, Flask	1.27 g/L	Not determined	Wang et al. 2017
Escherichia coli	5 g/L Glucose and 20 g/L Xylose	3,4-DHBA	Batch, Flask	0.38 g/L	Not determined	Gao et al. 2017
Escherichia coli	20 g/L Xylose	3,4-DHBA	Batch, Flask	7.71 g/L	60%	Liu et al. 2021
Saccharomyces cerevisiae	10 g/L glucose and 20 g/L Xylose	Glycolate	Batch, Flask	1.0 g/L	Not determined	Salusjärvi et al. 2017
Saccharomyces cerevisiae	10 g/L glucose and 10 g/L xylose	1,2,4-butanetriol	Batch, Flask	1,7 g/L	25%	Bamba et al. 2019
Saccharomyces cerevisiae	10 g/L glucose and 10 g/L xylose feeding glucose and xylose	1,2,4-butanetriol	Fed-batch, Bioreactor (pH ≥ 5.5)	6.6 g/L	57%	Yukawa et al. 2021
Saccharomyces cerevisiae	10 g/L glucose and 10 g/L xylose	3,4-DHBA, 3-HBL	Batch, Bioreactor (pH≥ 8.0)	6.5 g/L (3,4-DHBA) 0.2 g/L (3-HBL)	79%	This study

Fig. 1

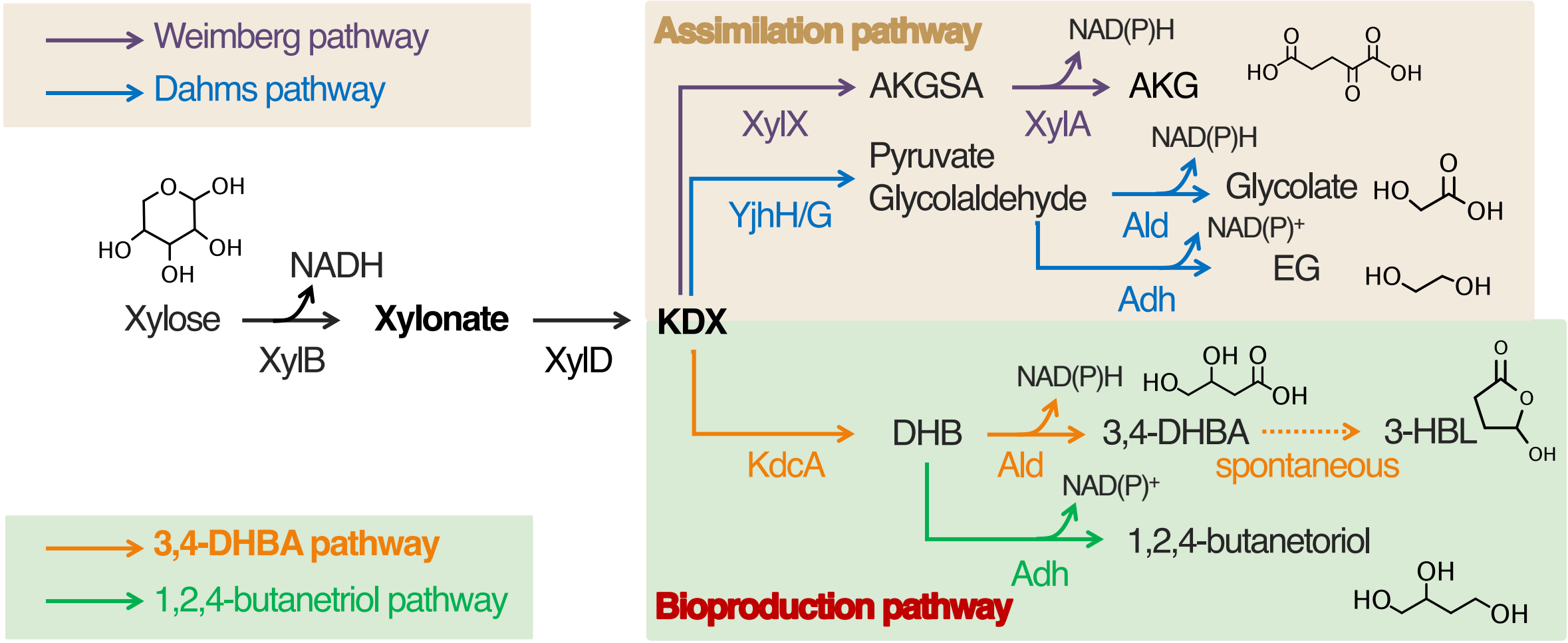
Weimberg pathway
Dahms pathway
3,4-DHBA pathway
1,2,4-butanetriol pathway
Xylose
NADH
XylB
Xylonate
XylD
KDX
Assimilation pathway
XylX
AKGSA
NAD(P)H
XylA
AKG
YjhH/G
Pyruvate
Glycolaldehyde
NAD(P)H
Ald
Glycolate
NAD(P)+
Adh
EG
KdcA
DHB
NAD(P)H
Ald
3,4-DHBA
spontaneous
3-HBL
NAD(P)+
Adh
1,2,4-butanetoriol
Bioproduction pathway

Figure 2

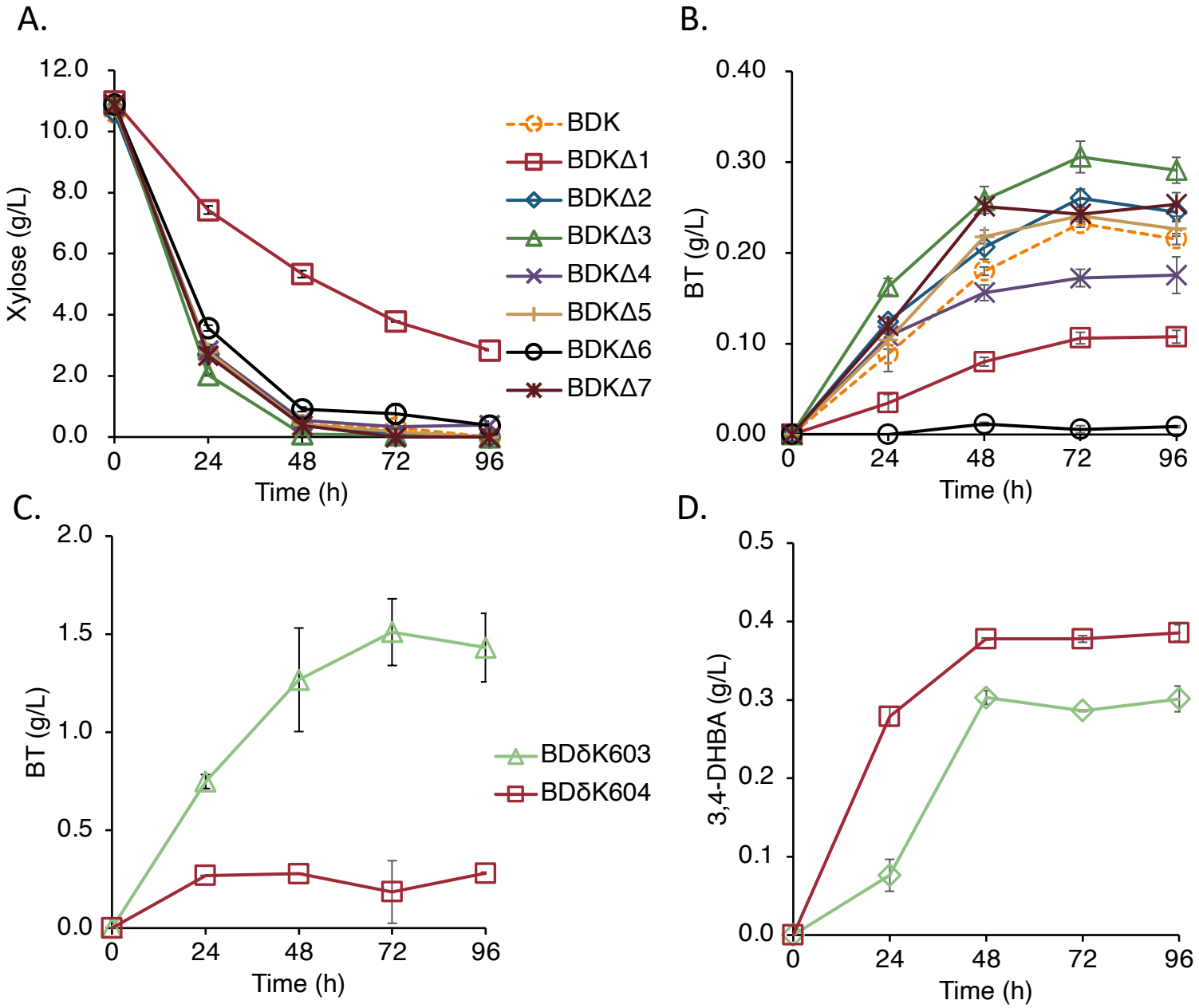
A.
Xylose (g/L)
12.0
10.0
8.0
6.0
4.0
2.0
0.0
0
24
48
72
96
Time (h)
BDK
BDKΔ1
BDKΔ2
BDKΔ3
BDKΔ4
BDKΔ5
BDKΔ6
BDKΔ7
B.
BT (g/L)
0.40
0.30
0.20
0.10
0.00
0
24
48
72
96
Time (h)
C.
BT (g/L)
2.0
1.5
1.0
0.5
0.0
0
24
48
72
96
Time (h)
BDδK603
BDδK604
D.
3,4-DHBA (g/L)
0.5
0.4
0.3
0.2
0.1
0.0
0
24
48
72
96
Time (h)

Figure 3

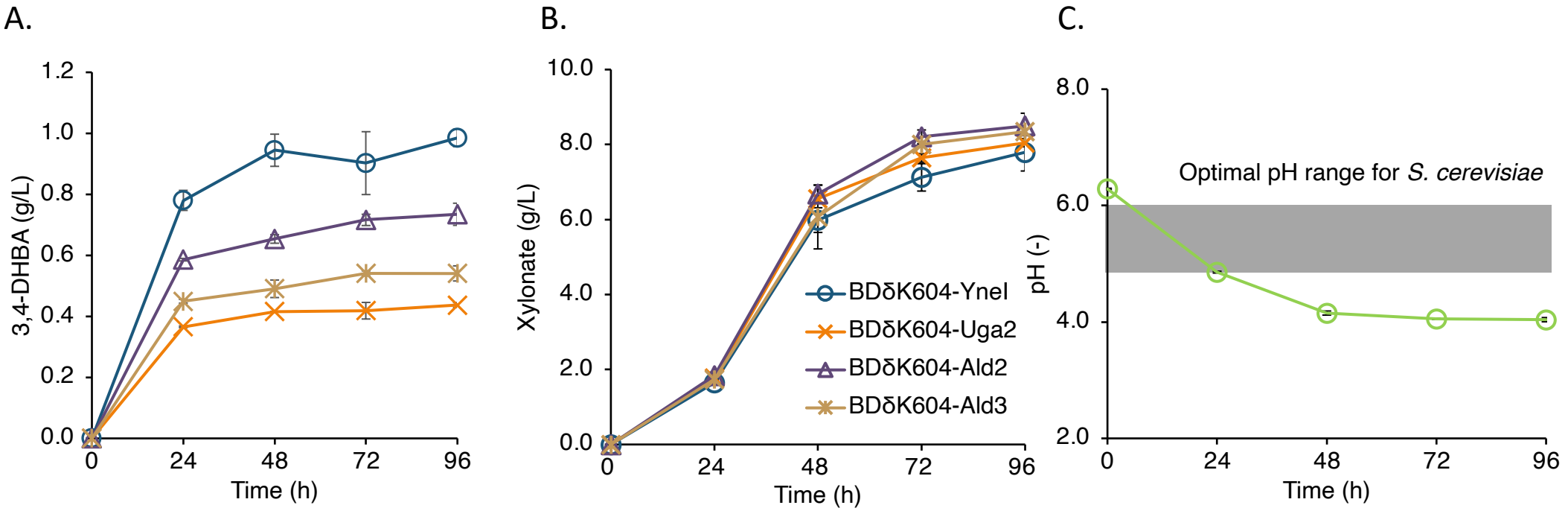
A.
3,4-DHBA (g/L)
1.2
1.0
0.8
0.6
0.4
0.2
0.0
0
24
48
72
96
Time (h)
B.
Xylonate (g/L)
10.0
8.0
6.0
4.0
2.0
0.0
0
24
48
72
96
Time (h)
BDδK604-YneI
BDδK604-Uga2
BDδK604-Ald2
BDδK604-Ald3
C.
pH (-)
8.0
6.0
4.0
2.0
Optimal pH range for S. cerevisiae
0
24
48
72
96
Time (h)

Figure 4

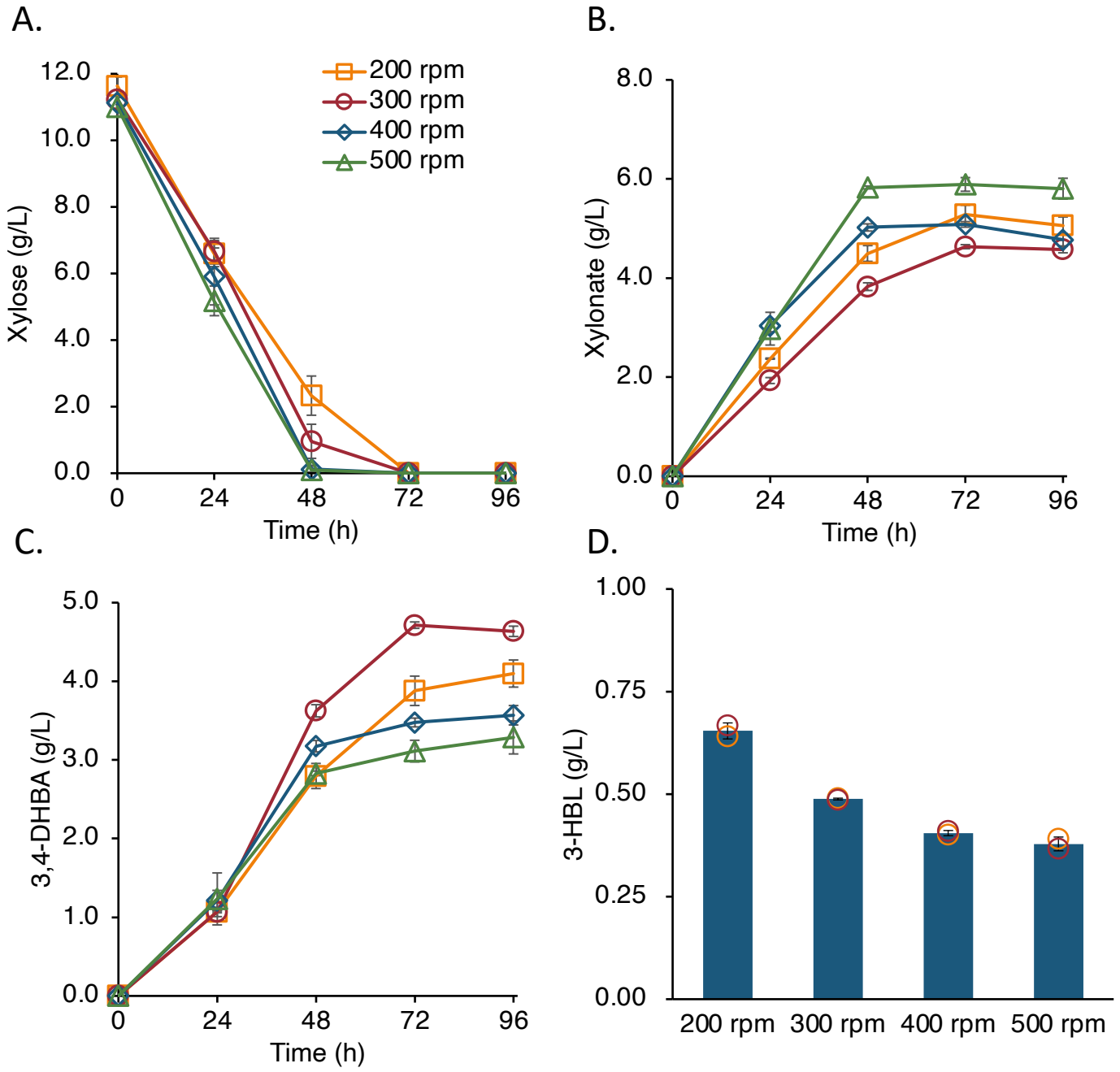
A.
B.
C.
D.
200 rpm
300 rpm
400 rpm
500 rpm
Xylose (g/L)
Xylonate (g/L)
3,4-DHBA (g/L)
3-HBL (g/L)
Time (h)
0
24
48
72
96
0.0
2.0
4.0
6.0
8.0
10.0
12.0
1.0
3.0
5.0
0.00
0.25
0.50
0.75
1.00

Figure 5

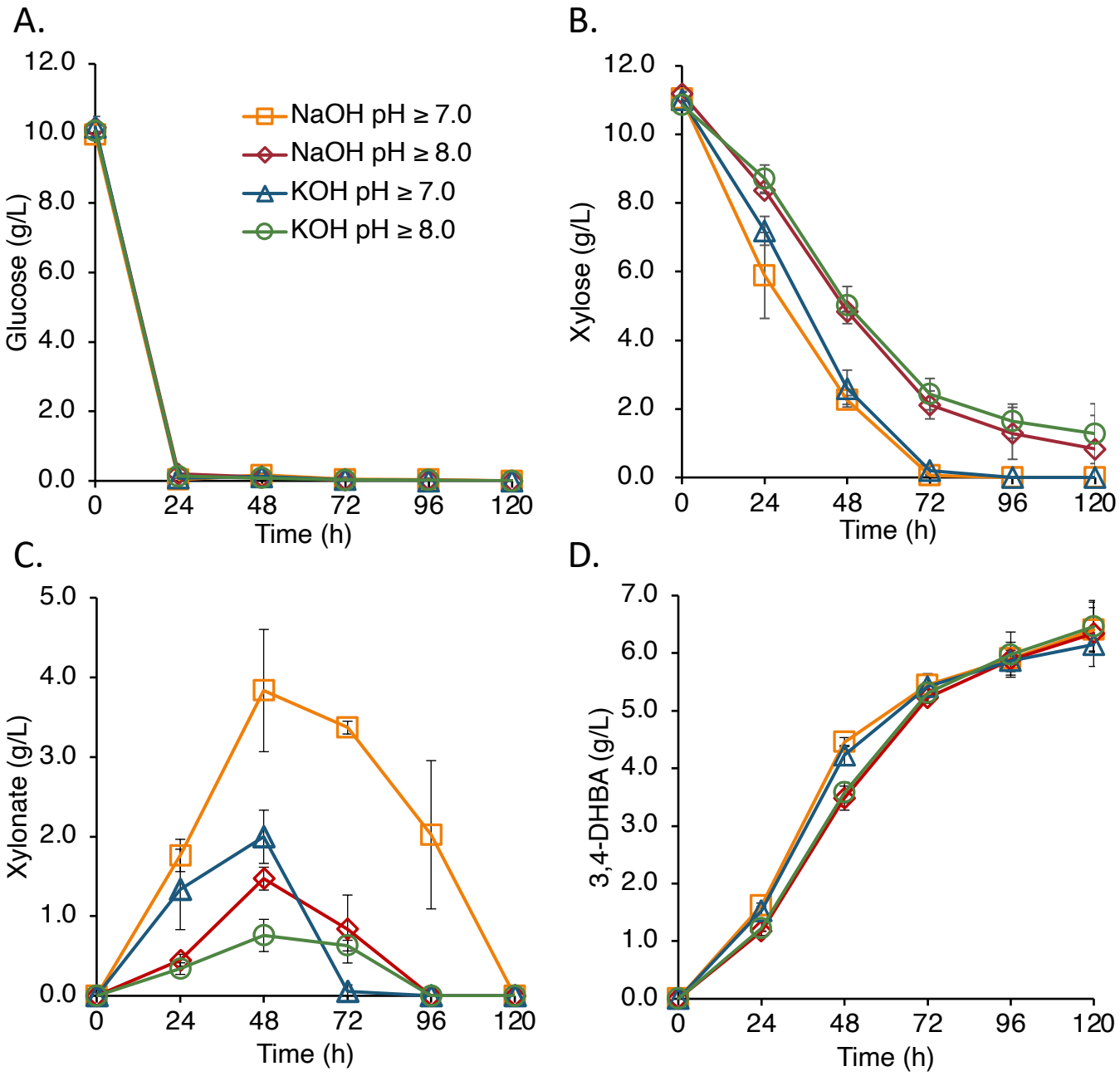
A.
B.
C.
D.
NaOH pH ≥ 7.0
NaOH pH ≥ 8.0
KOH pH ≥ 7.0
KOH pH ≥ 8.0
Glucose (g/L)
Xylose (g/L)
Xylonate (g/L)
3,4-DHBA (g/L)
Time (h)
0
24
48
72
96
120

Figure 6

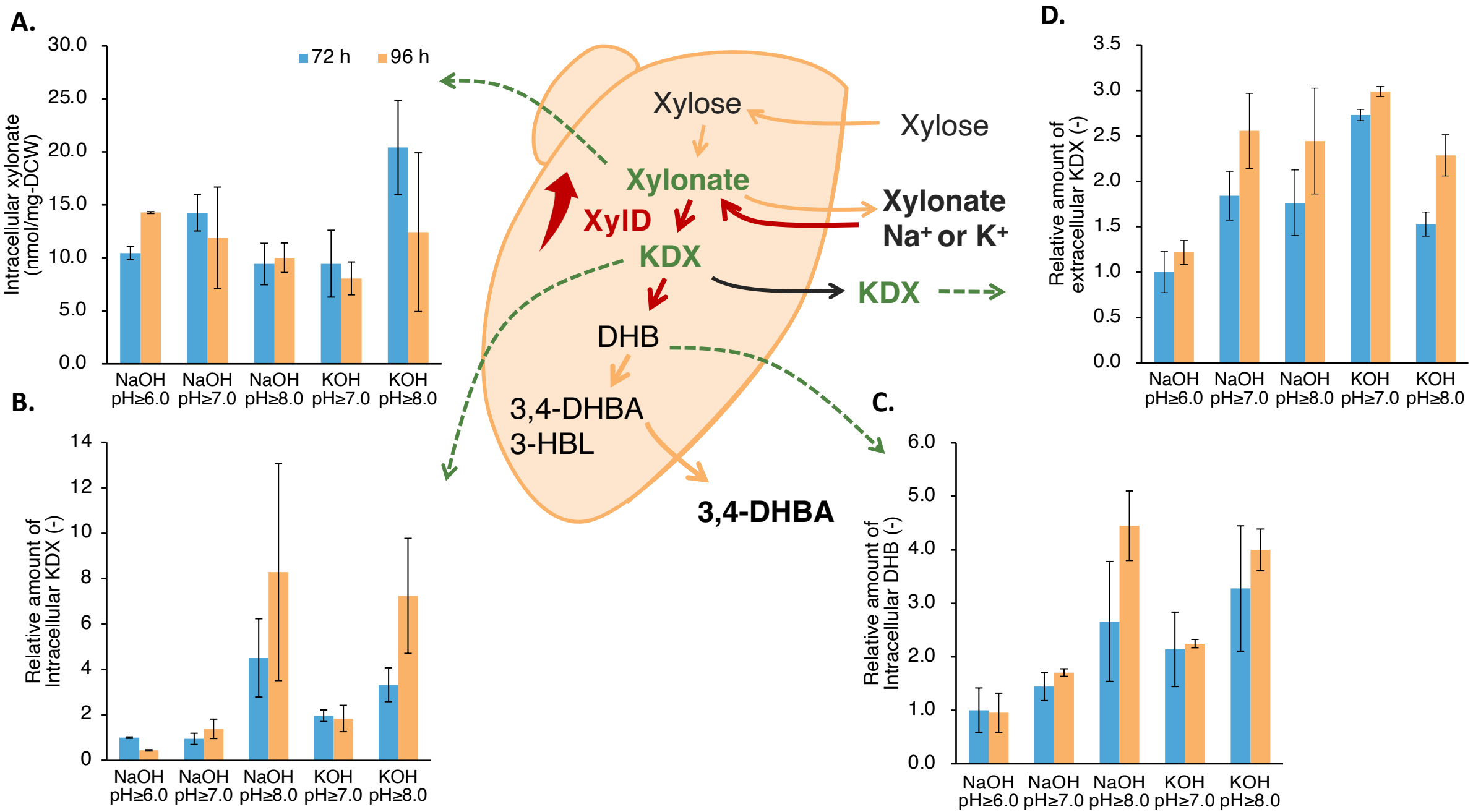
A.
Intracellular xylonate (nmol/mg-DCW)
72 h
96 h
NaOH pH≥6.0
NaOH pH≥7.0
NaOH pH≥8.0
KOH pH≥7.0
KOH pH≥8.0
B.
Relative amount of Intracellular KDX (-)
C.
Relative amount of Intracellular DHB (-)
D.
Relative amount of extracellular KDX (-)
Xylose
Xylonate
XylD
KDX
DHB
3,4-DHBA
3-HBL
Xylose
Xylonate
Na+ or K+
KDX
3,4-DHBA